IP/BBSR/94-8
Feb. '94

Fermilab Library
0 1160 0033484 1

— IP-BBSR-94-8 —

APR 8 19

COMPOSITION, SURFACE TOPOGRAPHY, STRUCTURE, RAMAN, ELECTROCHEMICAL AND PHOTOELECTROCHEMICAL SOLAR CELL STUDIES USING $Cd_xHg_{1-x}Te$ FILMS

S.N. Sahu*, M.J. Antonio+ and C. Sanchez++

* Institute of Physics, Sachivalaya Marg,
Bhubaneswar-751005, India

+ Departmento Q.A. Geology and Geochemistry
++ Departamento de Fisica Aplicada C-IV
Universidad Autonoma de Madrid
Cantoblanco, 28049 Madrid, SPAIN

ABSTRACT

Cd-rich $Cd_xHg_{1-x}Te$ films have been electrodeposited under potentiostatic conditions on conducting glass and Ti substrates from an acidic solution containing the respective ions as $Cd^{2+} : Hg^{2+} : HTeO_2^+ = 100 : 1 : 2$. Six films one after another have been prepared from a single electrochemical cell. EDAX analysis of the air annealed films show decreasing Hg content in the deposit as the number of film preparation increases. SEM analysis indicate undulatory surface with Hg-rich clusters at the top surface. XRD analysis indicate the presence of $Cd_xHg_{1-x}Te$ along with CdTe/HgTe. The $Cd_xHg_{1-x}Te$ alloy formation have been confirmed from Raman shift measurements which change with composition, x. Electrochemical characterizations indicate the as-deposited films are n-type but converts to p-type after air annealing. Spectral response measurements gave band gap values that change with Hg content in the deposit. Band gap values ranging from 1.1 eV to 1.45 eV have been estimated. Photoelectrochemical solar cells using polysulfide electrolyte have been fabricated which gave an open circuit photovoltage and short circuit photocurrent respectively as 325 mV and 5.5 mA/cm^2 under 60 mW/cm^2 intensity of illumination.

1.0 INTRODUCTION

The near optimum band gap and high absorption coefficient associated with Cd makes it ideally suitable for solar cell application[1]. The efficiency of CdTe solar cell c further be improved by incorporating low quantity of Hg forming Cd-rich Cd_xHg_{1-x} (CMT) alloy. Incorporation of Hg in to CdTe may slightly lower the photovoltage b the photocurrent may increase considerably which would increase the efficiency of CM as compared to CdTe. Depending upon the Hg content in the CMT alloy, two possib applications viz. photovoltaic cells[2,3] and photodetectors[4,5] emerge. Further, the ba gap of CMT can be varied from 0.1 to 1.5 eV for x changing from 0.1 to 1.0. However, f photovoltaic purposes, the range of band gap of interest is 0.9 to 1.5 eV which correspon to the composition range $0.7 < x < 1.0$. Thin films of CMT for solar cells have speci advantage that it minimizes the material wastage and cost. A CMT film of 1.0 μm thi should be good enough for required amount of photon absorption. Various methods f preparing CMT films have been described in literature. They include laser ablation vacuum evaporation[7-9], MBE[10], sputtering[11] and MOVPE[12]. Although these are bett methods to prepare Hg-rich CMT films but appears to be not cost effective if one interested to prepare Cd-rich CMT for photovoltaic purposes. However, electrodepositi technique which is simple, less expensive and less polluting can easily be employed prepare both binary and ternary[15,16] semiconductor compounds. Earlier work on Cd-ri CMT electrodeposition is due to Basol and Tseng[2], Sahu and Sanchez[17], Newmann-

Spalart et al[18] and Ortega[19] but not much details have been reported. The present work describes the electrodeposition of CMT films and their subsequent characterizations.

2.0 EXPERIMENTAL

2.1 Film Preparation

The electrochemical cell for electrodeposition of CMT film consists of a Ti-cathade, Pt-anode, saturated calomel electrode (SCE) with respect to which the voltages were measured and an aqueans electrolyte containing $CdSO_4, HgSO_4$ and TeO_2 in their respective ionic concentration as $Cd^{2+} : Hg^{2+} : HTeO_2^+ = 100 : 1 : 2$. The procedure for substrate cleaning, solvent preparation and purification are being described in detail elsewhere[20]. Electrodeposition was being carried out with varied pH, electrolysis temperature, cathodic bias and ionic concentrations of the constituent elements. Reasonably good CMT films were prepared within 12 minute at pH = 1.6, electrolysis temperature = 100°C. The potential region for three ionic species were determined by drawing polarization curves using a potentiostat model 105 (HQ Instruments) and found to be -0.65 V_{SCE}. As the deposition potentials of the respective elements are wide apart[22], being more positive for Hg and more negative for Cd, very low and very high concentrations of Hg^{2+} and Cd^{2+} and slightly higher concentration of $HTeO_2^+$ were taken in the electrolyte. As Hg^{2+} and $HTeO_2^+$ specieses are more noble than Cd^{2+}, during deposition the more noble specieses are more likely to be depleted from the cathode electrolyte interface. Hence, the deposition was carried out under stirred condition. Being the low solubility of TeO_2 in H_2SO_4, hot KOH (pH = 12.3) was being used as a solvent for TeO_2 dissolution. One of our motivation was to prepare large number of CMT films from the parent single electrochemical cell. Hence, each time, two Ti substrates of each area 1 cm^2 were dipped in the electrolyte of which both the front and back surfaces were uncovered. CMT films were prepared six times from the same electrolyte using two substrates at a

time for a time duration of 12 minute each. In this way the effective area over 24 cm^2 have been deposited. The CMT films were then washed with fine water jets, dried and post annealed in air at 300°C for 20 minute. The annealed samples were then subjected to different characterizations.

2.2 Characterizations

The composition and surface topography of the CMT films have been analysed by a Philips Scanning Electron Microscope (SEM) - 500 equipped with a microanalyser (EDAX). The back ground signal, electronic noice and matrix effects were corrected by a ZAF programme and spectra were collected. The gain callibration was routinley carried out using Cu as standard. The concentrations of different elements present in CMT films have been estimated in terms of weight percentage. The EDAX results represent the average over atleast three regions of the sample and within ±5% error. The SEM pictures were taken for surface topography analysis using a polaroid camera attached to the Philip SEM-500.

Structural identifications were carried out using Siemans Diffractometer D-500. The lattice spacing (d-values) were calculated for different diffraction angle, 2Θ and compared with standard data from JCPDS[21] file. For XRD analysis, CMT films deposited over Ti were as such used.

Because of similar lattice spacing values of $CdTe, HgTe$ and CMT, it is difficult to conclude the CMT alloy formation from XRD analysis alone. Hence, Raman shift measurements were carried out at room temperature for some typical films. Raman experiments were performed in the back scattering configuration using the wavelength, $\lambda = 5145.A^0$ from a Ar^+ laser ($< 25mW$). Raman shifts were noted for different CMT composition and were compared with literature data. For Raman experiments CMT samples deposited on Ti were as such used.

Electrochemical characterizations in dark and under illumination ($He-Ne$ laser, $\sim 10mW$) were carried out in $0.5M\,Na_2SO_4$ electrolyte using a potentistat (EG and G model 362) inorder to test the type of conductivity of the annealed CMT films.

Spectral response tests of the CMT samples were carried out in 0.5 M Na_2SO_4 electrolyte using a three electrode one compartment cell comprising Ti/CMT as working electrode, Pt as counter electrode and saturated calomel electrode as the reference electrode. The experimental arrangement for spectral response measurement is shown in figure 1. This consists of a light source, I.R. filter, a lense to focus the light beam to the monochromator (Jovin Yuon Division d'Instruments, S.A. monochromator), a light chopper (EG and G model 199), a filter and a lence to focus the light beam on the working electrode (through a quartz window) dipped in the electrolyte. The working electrode was biased to -0.5 V_{SCE} through a potenitiostat (EG and G model 362 scanning potentiostat) and the output is fed to a lock-in-amplifier (EG and G model 5104) and X-Y recorder. The negative bias was applied to the CMT films due to their p-type behaviour as evidensed from electrochemical measurements. The as-deposited CMT films are n-type. The spectral response measurements have been done inorder to determine the band gap and quality of the CMT films.

Photoelectrochemical solar cells (PESCs) were fabricated using an agueous electrolyte containing $Na_2S.9H_20(2M)$, $NaOH(1M)$ and S(3M). Pt was being used as a counter electrode. The light intensity was adjusted to $60mW/cm^2$. The photovoltage and photocurrent were measured under different load conditions from the $PESC_s$ fabricated in the above manner.

3.0 EXPERIMENTAL RESULTS AND DISCUSSION

3.1. Compositional analysis:

EDAX analysis were carried out to estimate the composition of six CMT films

prepared from the single electrochemical cell and is shown in figure 2 in terms of Cd/Hg, (Cd+Hg)/Te and Hg/Te ratios as a function of number of films. Note that the Hg content in the deposit decreases with the increasing number of films. Similar is the case with (Hg+Cd) content in the deposit. However, in both the cases some irregularity is seen after the fourth film in which case there is an increase in Hg or (Hg+Cd) content in the deposit. The reason for this iregularity is not known. However, we believe, this might be due to the disturbance in the stirring rate or effect of change in deposition potentials of the constituent elements. In any case there is a constant decrease of Hg content in the deposit as the number of film preparation increases. SEM analysis (to be discussed later) indicates the presence of Hg-rich clusters at the top surface of the film. The Hg content in the underlying films are found invariably lower than the clusters. Typical EDAX pictures of six CMT films are shown in figure 3 which indicate the presence of all the three elements viz. Cd. Hg and Te in the CMT deposit. In order to know the reason of the Hg-rich clusters, we need to know the deposition potentials of individual elements which are as:

$$Cd(s) = Cd^{2+} + 2e^- = -0.403V + 0.0295ln(a_{Cd^{2+}}/a_{Cd})$$

$$Hg(s) = Hg^{2+} + 2e^- = +0.905V + 0.0295ln(a_{Hg^{2+}}/a_{Hg})$$

$$Te(s) + 2H_20 = HTeO_2^+ + 3H^+ + 4e^- = +0.551V - 0.0443pH + 0.0148ln(a_{HTeO_2^+}/a_{Te})$$

The deposition potentials are expressed with respect to Normal Hydrogen Electrode. Cd(s) etc. are the solid deposit. a_{Cd} etc. are ionic activities in the solid deposit (taken as unity) and in the bulk electrolyte. The deposition potential of Hg is highly positive and nobler than Te. The deposition potential of Cd is highly negtive and less noble as compared either to Hg or Te. Hence, for co-deposition of three elements, the activities, vis-a-vis the ionic concentrations are to be adjusted such that their deposotion potentials

are brought closer. For this reason, very high and very low concentrations of Cd^{2+} and Hg^{2+} and relatively higher concentrations $HTeO_2^+$ were taken in the electrolyte. As Hg^{2+} has a high positive potential, first deposition and depletion of Hg^{2+} at the cathode-electrolyte interface is expected. This would result a decrease in Hg content in the subsequent number of films prepared from the same electrolyte. Further, this feature would give better nucleation facilities for more Hg deposition favouring a Hg-rich cluster at the top surface of the film. At a stage when the Hg-depletion is too much, than Te deposition would be favoured. Hence, for CMT deposition both Hg^{2+} and $HTeO_2^+$ become the rate determining species.

3.2 Surface topography analysis:

Surface feature of typical CMT films were determined by SEM analysis shown in figure 4. Typical undulatory surface with Hg-rich clusters are seen. The surface roughness and the Hg-rich clusters per unit area of the film decreases with the increasing number of CMT films prepared from the single electrolytic cell. EDAX analysis of clusters and the underlying films indicate a higher Hg content in the clusters as compared to the underlying film. The exact reason for the cluster formation is not known. However, we believe that it might be the effect of surface roughness. If the substrate surface is not well polished, then, it contains more sites on those surface regions protruding towards the anode. On passing a voltage/current, the local current density at those protruding surfaces would be higher than other regions which would give rise to faster nucleation and growth at those sites. As Hg^{2+} species is the noblest of all the three elements present in the electrolyte and have high positive deposition potential, formation of Hg-rich clusters at the top surface cannot be rulled out. CMT films with high Hg-rich clusters are also seen by other workers[22]. The first CMT film was found to have most of the surface covered with Hg-rich clusters, hence, it was discarded. Subsequent characterizations

were carried out with other five CMT films.

3.3. Structural analysis:

X-ray diffraction patterns of different number of CMT films (corresponding to thier Cd/Hg ratios in the deposit) prepared from a single electrochemical cell is shown in figure 5. Note that along with cubic CMT extraneous compounds/elements viz CdTe, HgTe and unreacted Te are detected. The relative X-ray intensities of different CMT films are indicated by their respective Cd/Hg ratios in the deposit along with prominant X-ray intensities of CdTe shown in figure 6. It can be noted that the (111) peak is always the most intense for all the films suggesting the existence of strong preferred orientation. Besides the (111) orientation, the (220) and (311) peaks are also reproducible for all the films although other relatively weak peaks viz (331), (400) and (422) are also detected. We did not observe a strong preferred orientation for very high or very low concentration of Hg in the deposit as was the case with other workers[18]. Further, we observe a gradual increase in intensity ratios of (111) to (220) with increasing number of films or decreasing Hg content in the deposit. The CMT film for which the Cd/Hg ratio is 1.806, the peak intensity ratio of (111) to (220) is 1.64:1. This value increases with increasing number of films. The fourth film for which the Cd/Hg ratio is 1.432, the (111) to (220) intensity ratio is 1.92:1. The fifth film is again cluster rich as seen from SEM picture gave the (111) to (220) intensity ratio as 1.66:1. For normal random powder CMT sample, the (111) to (220) intensity ratio is 1:1 and for better oriented CMT sample, the value is 100:1. So, we believe that our CMT films are not better oriented as compared to the CMT films prepared by laser oblation[6].

3.4 Raman studies:

Raman studies at room temperature for some typical CMT films (film Nos.2,3,4)

are carried out using Ar^+ laser ($< 25mW$) and the spectra are shown in figure 7. Note that there is a shift in Raman frequency with composition, x which agree reasonably well with the reported data[23]. Raman shifts at 144 cm^{-1} and 126 cm^{-1} for x = 0.6, 142 cm^{-1} and 124 cm^{-1} for x = 0.74 and 143 cm^{-1} and 125 cm^{-1} for x = 0.77 corresponding to the transverse optical (TO) phonons of CMT have been identified. This confirms the formation of CMT alloy in the electrodeposit.

3.5 Electrochemical characterizations:

Figure 8 shows the voltammograms of two typical annealed CMT films (fig.8b and c) in dark and under light. The dark characteristic (fig.8a) is the representative of both the films. In both the cases, a photocathodic current indicated the p-type behaviour of CMT films. However the fifth films (fig.8c) shows a higher photocathodic current as compared to the third (fig.8b) CMT film. The higher photocathodic current (fig.8c) is due to reduction in Hg-rich clusters at the top sruface of the film. All the asdeposited CMT films show n-type behaviour but converts to p-type after air annealing in agreement with other reported results[3,18].

3.6 Spectral response studies:

Figure 9 shows the spectral response curves at room temperature of different number of films prepared from the single electrochemical cell. Note that the very low photocurrent is associated with highly Hg-rich clustered CMT film (fig.9a). The photocurrent yield increases with increasing number of films or decrease in Hg-rich clusters in the film. Infact, the Hg-rich clusters act as recombination centres of the semiconductor electrolyte junction device which short circuit the current path and lowers the photocurrent yield. Another feature is that as the number of film preparation increases, the fundamental absorption edge shifts towards lower wave length absorption. This can be attributed to

the lowering of Hg or increase in Cd content (as seen from EDAX results) in the deposit which ultimately lowers the band gap of CMT alloy. Some departure is seen with the fifth (Fig.9D) film from the general trend of increasing towards lower wavelength response. This departure is also seen in EDAX analysis (fig.2). Most of the spectral response curves show shouldering/humps which are due to water absorption[24]. From the spectral response curves one can see that there is a fall of spectral response (decreasing photocurrent yield) towards lower wavelength side which can be attributed to the diffusion of photogenerated majority carriers to the interface followed by subsequent recombination with photogenerated minority carriers[25]. As the CMT is a direct band gap semiconductor, the band gap can be estimated from the extrapolation to zero absorption in the $(I_{ph}h\nu)^2$ Vs $h\nu$ plot shown in figure 10. Band gap values ranging from 1.12 eV to 1.45 eV have been estimated for different CMT films. Attempts have been made to calculate the band gap theoretically for different x values from the relation[26].

$$Eg(eV) = -0.303 + 1.984x - 0.654x^2 + 0.579x^3 + 10^{-4}T(5.5 - 13.92x + 5.84x^2)$$

where T is the absolute temperature. The Eg values are calculated at room temperature. However, the calculated band gap values are found not to agree well with the experimentally determined one. The descripancy may be either due to the non-uniformity in the surface/composition or the inaccuracies in EDAX technique used for composition estimation.

3.7 Photoelectrochemical solar cells (PESCs)

Photoelectrochemical solar cell using the sixth film ($E_g = 1.45eV$) have been fabricated using a polysulfide electrolyte having the cell configuration as $Ti/CMT/S^{2-}$, S_2^{2-}/Pt. The photocurrent and photovoltages were measured under different load conditions and is shown in figure 11. Energy conversion efficiency of 1.1% with a fill factor

37% have been achieved from such type of cell which is lower than the reported results[2,3]. The reasons for the poor efficiency is mainly due to the presence of Hg-rich clusters at the surface which particularily lowers the photocurrent. Infact, short time etching of the CMT samples in dil $H_2SO_4(2:50 = H_2SO_4 : H_20)$ improves the photocurrent. This study is in progress.

4.0 CONCLUSION

A large number of CMT-semiconductor films have been electrodeposited from a single electrochemical cell. The Hg composition in the CMT film decreases as the number of film preparation increases which results in the lowering of Hg-rich clusters at the surface evidensed from SEM analysis. Structural identification reveals the presence of cubic CMT along with CdTe/HgTe in the deposit. The formation of CMT alloy in the deposit have been confirmed from Raman frequency measurements. The as-deposited CMT films are n-type but converts to p-type after air annealing. Band gap values ranging from 1.12 eV to 1.45 eV have been estimated from spectral response measurements using different composition, x of CMT films. Photoelectrochemical solar cells fabricated using a polysulfide electrolyte gave energy conversion efficiency $\sim$ 1.1% with a fill factor of 37%.

5.0 ACKNOWLEDGEMENTS

The financial assistance received by one of the authors (S.N.S) to carry out a major part of this work from the Ministerio de Educacion Ciencia (Spain) is gratefully acknowledged.

REFERENCES

1. K.W. Mitchell, "Evaluation of the CdS/CdTe heterojunction solar cells" (Garland, New York, 1979) and the references therein.
2. B.M. Basol and E.S. Tseng, Appl. Phys. Lett. **48**, 946 (1986).
3. C. Levy-Clement, R. Triboulet and R. Tenne, Solar Energy Mater, **17**, 201 (1988).
4. M.B. Reine, A.K. Sood and T.J. Tredwekk, Semiconductors and Semimetals, R.K. Willardson and A.C. Beer, eds.(Academic Press, New York, 1981) Vol.18 p.201.
5. R. Dornhaus and G. Nimtz, "In Narrow gap semiconductors", D. Dornhaus, G. Nimtz and B. Schlicht, eds., (Springer-Verlag, Berlin, 1983) p.119.
6. J.T. Cheung and D.T. Cheung, J. Vac. Sci. Technol. **21**, 182 (1982).
7. R.F.C. Farrow, G.R. Jones, G.W.Williams, P.W. Sullivan, W.J.O. Boyle and J.T.M. Wotherspoon, J. Phys. D. Appl. Phys. **12**, L117 (1979).
8. S.A. Ignatowicz, Thin solid films, **6**, 299 (1970).
9. D.K. Hohnke, H.Holloway, E.M. Logothetis and R.C. Crawley, J. Appl. Phys. **12**, 2187 (1971).
10. M.H. Francombe, S.V. Krishnaswamy, A.J. Noreika, W.J. Takel, T.A. Temofonte and J.H. Rieger, Thin Solid Films **168**, 307 (1989).
11. H. Kraus, S. Parker and J.P. Smith, J. Electrochem. Soc. **114**, 616 (1967).
12. V. Natarajan, N.R. Taskar, J.B. Bhat and S.K.Chandhi, J. Electron. Mater **17**, 179 (1988).
13. M.P.R. Panicker, M. Knaster and F.A. Kröger, J. Electrochem. Soc. **125**, 566 (1978).
14. S.N. Sahu, J. Mater Sci. Mater - in Electronics, **3**, 102 (1992).
15. S.N. Sahu, R.D.L. Kristensen and D. Haneman, Solar Energy Mater, **18**, 235 (1989).
16. R.N. Bhattarya, J. Appl. Electrochem. **16**, 168 (1986).

17. S.N. Sahu and C. Sanchez, Solid State Commun. **73**, 597 (1990).

18. M. Neumann - Spallart, G. Tamizhamani, A. Boutry-Forveille and C. Levy-Clement. Thin solid films, **169**, 315 (1989).

19. J. Ortega, An. Quim, **88**, 459 (1992).

20. S.N.Sahu and C. Sanchez, Spain Potent No.8902715 (1989).

21. JCPDS; Joint Committee for Powder Diffraction file for Inonganic Materials (1979).

22. B.M. Basol, E.S. Tseng and O.M. Stafsudd, Proc. 18th IEEE photovoltaic specialist conf. Lasvegas (1985).

23. J. Baars and F. Sorger, Solid State Commun. **10**, 875 (1972).

24. J.L. Schmit and E.L. Stelzer, J. Appl. Phys. **40**, 4865 (1969).

25. J. Reichman, Appl. Phys. Lett. **38**, 251 (1981).

26. R. Legros and R. Triboulet, J. Cryst. Growth, **72**, 264 (1985) Erratum. J. Cryst. Growth, **78**, 168 (1986).

FIGURE CAPTIONS

Fig.1. Experimental arrangement for spectral response measurement.

Fig.2. Atomic ratios of Hg/Te, (Cd+Hg)/Te and Cd/Hg as a function of the number of CMT films prepared from a single electrolytic bath.

Fig.3. EDAX photographs of six CMT films prepared from a single electrolytic bath. The film numbers are indicated in the photographs.

Fig.4. SEM photographs of some typical CMT film. (a) No.2 (b) No.3, (c) No.5, (d) No.6 and (e) cross section showing the Ti substrate and the CMT layer.

Fig.5. X-ray diffraction patterns of different CMT films. Corresponding Cd/Hg ratios of each film are indicated.

Fig.6. X-ray peak intensitites of different CMT films. Corresponding Cd/Hg ratios of each film are indicated.

Fig.7. Raman spectra of some typical CMT film. The composition of the CMT films are indicated.

Fig.8. Cyclic voltammograms of some typical CMT film in dark and light (a) dark characteristic, (b) and (c) characteristics under light.

Fig.9. Photocurrent Vs photon wavelength of different CMT films obtained from spectral response measurements. A,B,C,D and E corresponds to film numbers 2,3,4,5 and 6 respectively.

Fig.10. $(I_{ph}h\nu)^2$ Vs $h\nu$ plots of different CMT films derived from figure.9. A,B,C,D and E corresponds to film numbers, 2,3,4,5 and 6 respectively.

Fig.11. Photocurrent Vs photovoltage characteristic under different load condition obtained from a PESC with configuration Ti/CMT/S^{2-}, S_2^{2-}/Pt.

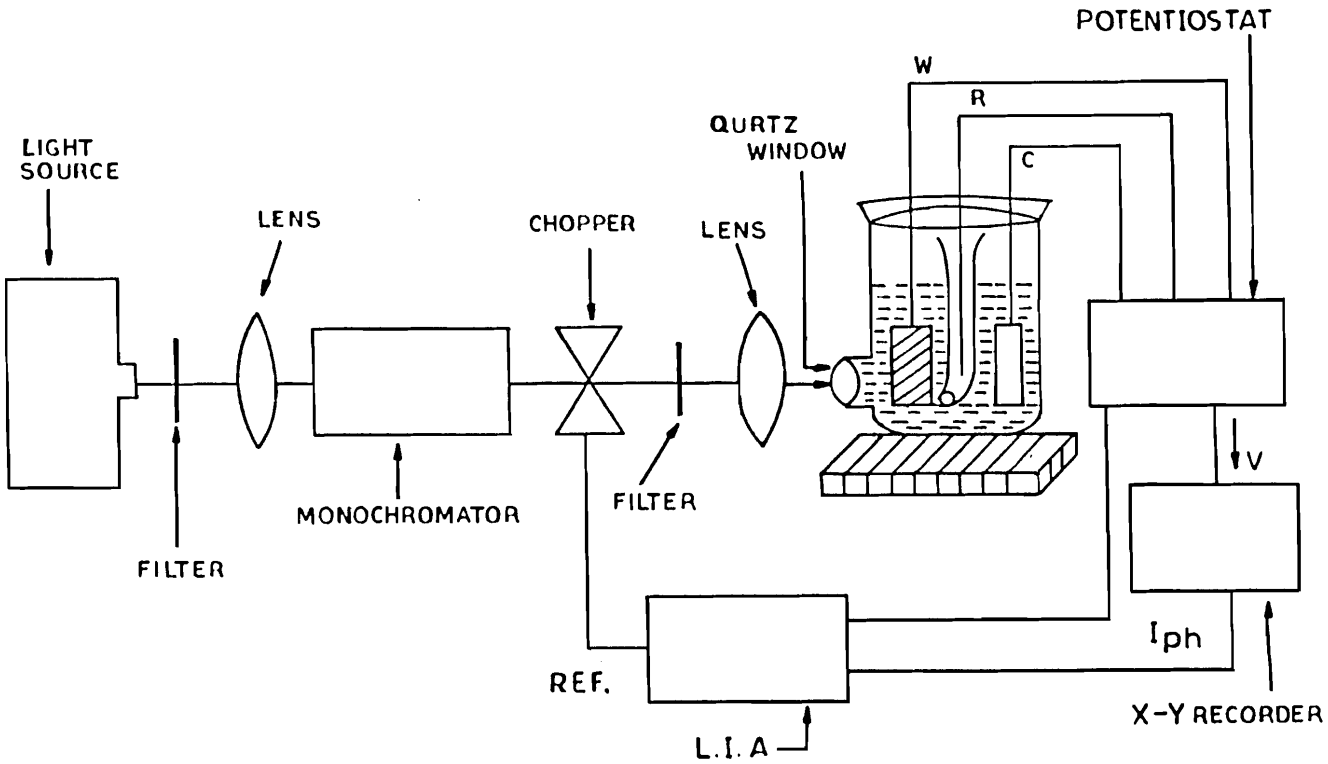
POTENTIOSTAT
W
R
C
QURTZ WINDOW
LIGHT SOURCE
LENS
CHOPPER
LENS
V
MONOCHROMATOR
FILTER
FILTER
Iph
REF.
X-Y RECORDER
L.I.A

Fig.1

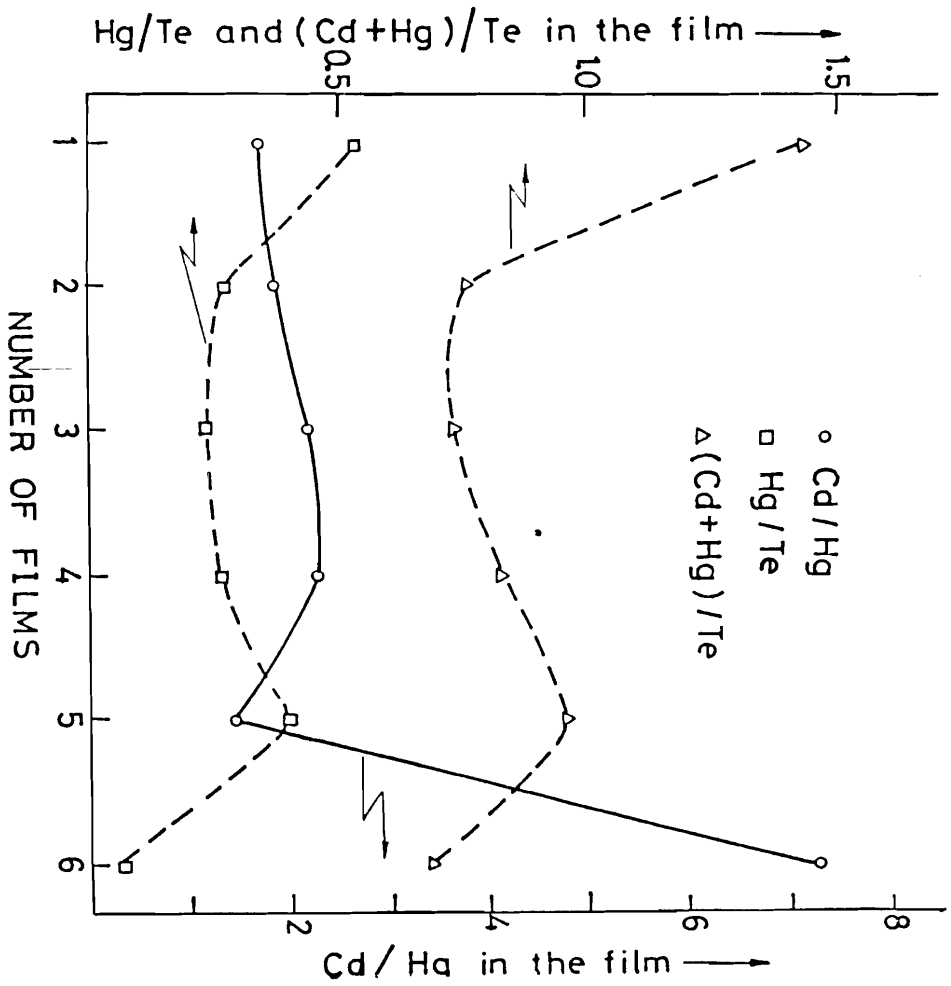
Hg/Te and (Cd+Hg)/Te in the film
0.5
1.0
1.5
NUMBER OF FILMS
1
2
3
4
5
6
Cd/Hg
Hg/Te
(Cd+Hg)/Te
2
4
6
8
Cd/Hg in the film

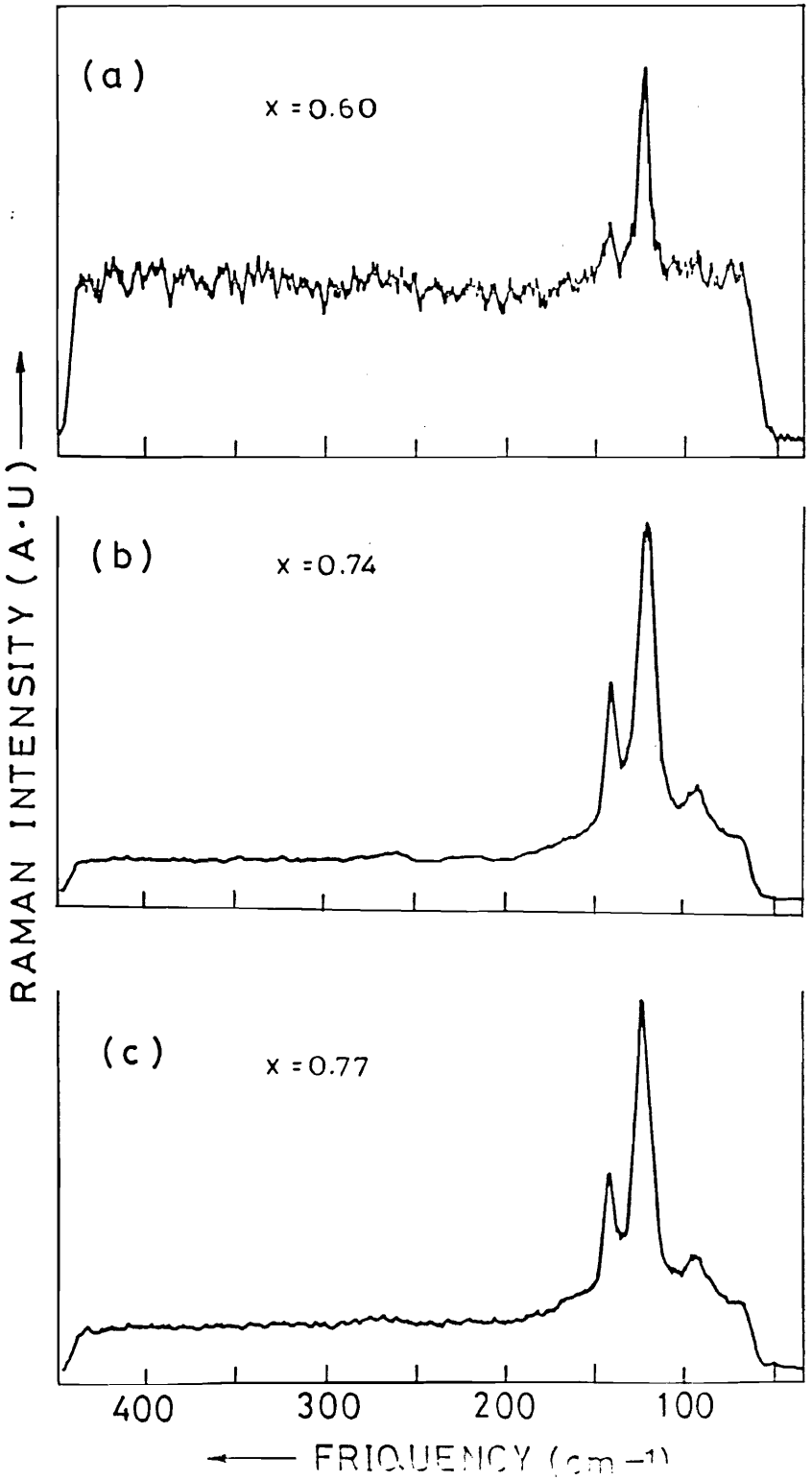

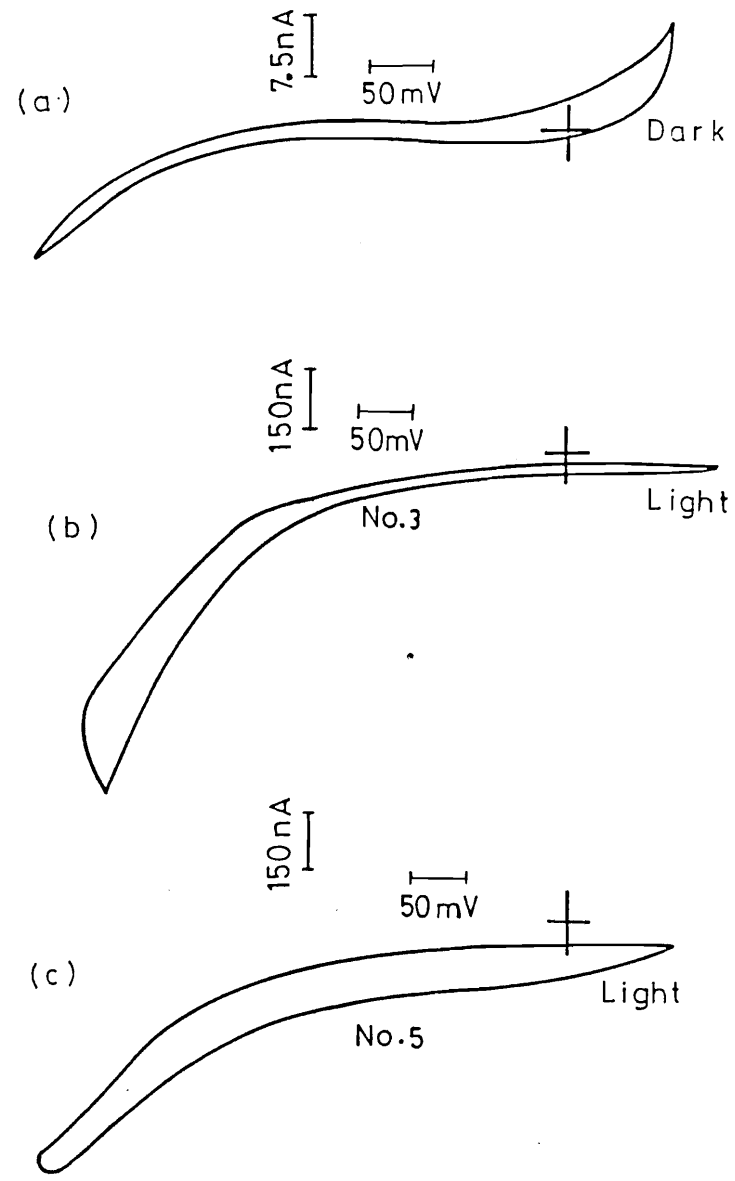

Scan rate for a, b and c:10 mV/s

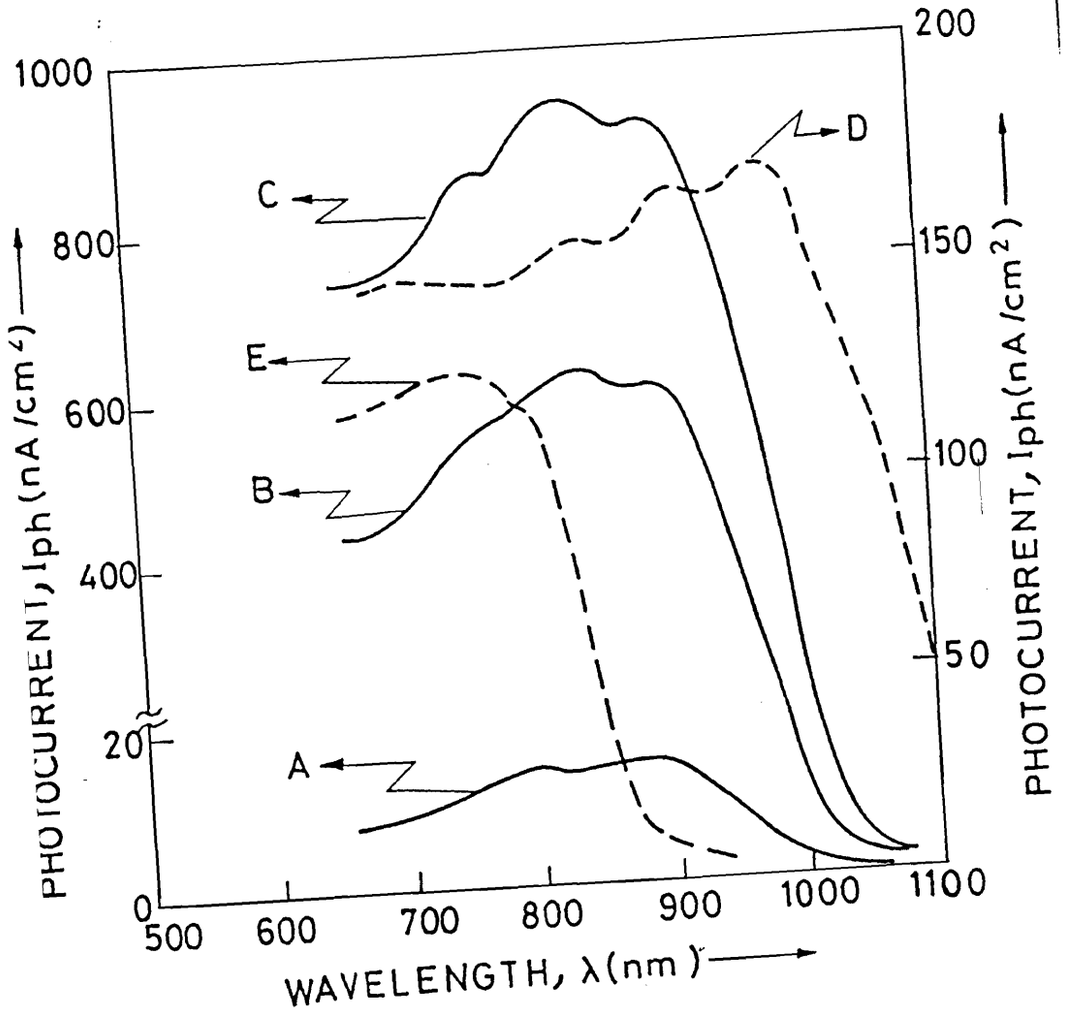
PHOTOCURRENT, Iph (nA/cm²)
PHOTOCURRENT, Iph(nA/cm²)
WAVELENGTH, λ(nm)
A
B
C
D
E
0
20
400
600
800
1000
50
100
150
200
500
600
700
800
900
1000
1100

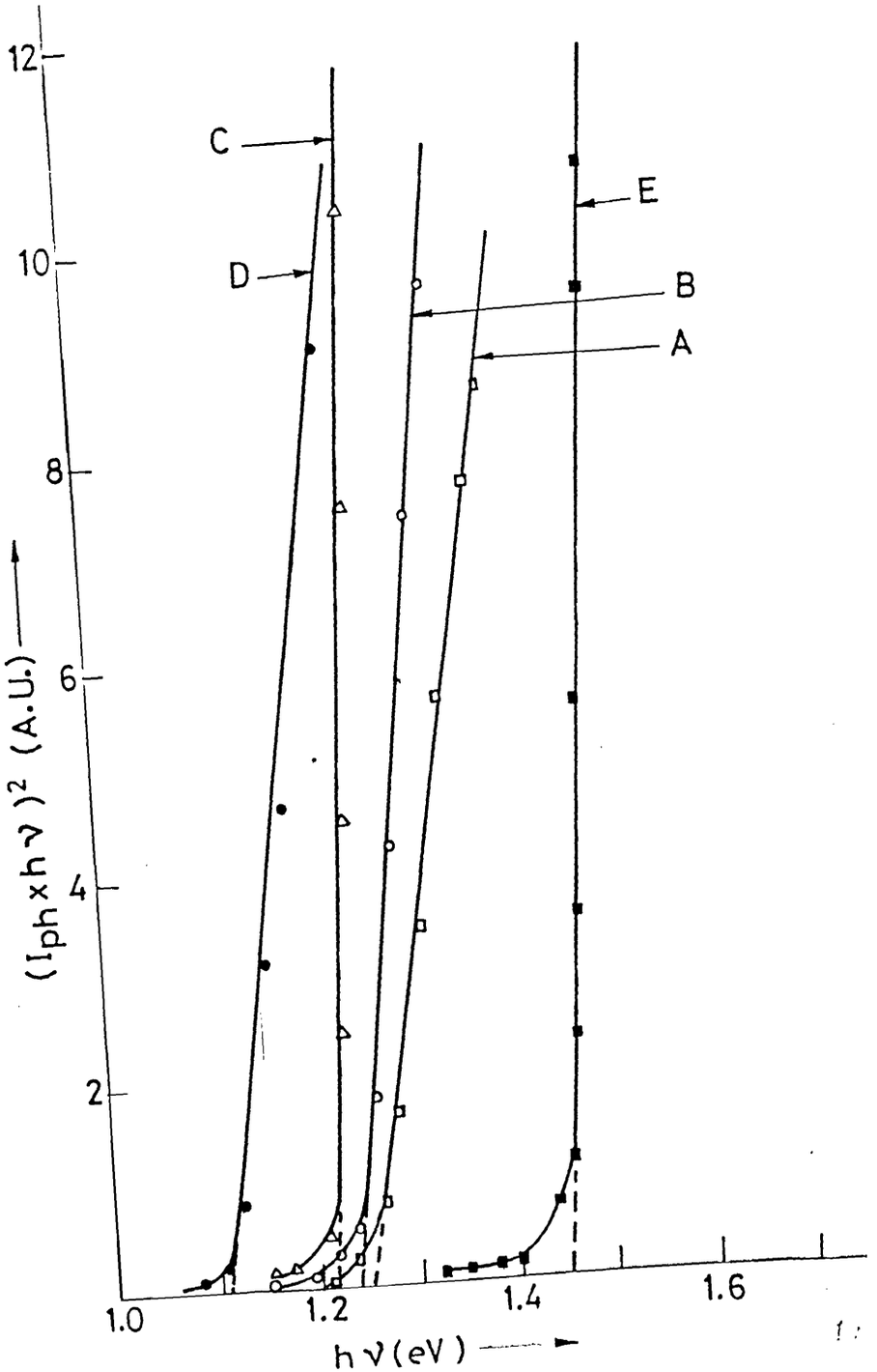
(Iph x hν)² (A.U.)
hν (eV)
A
B
C
D
E
2
4
6
8
10
12
1.0
1.2
1.4
1.6

Fig.9

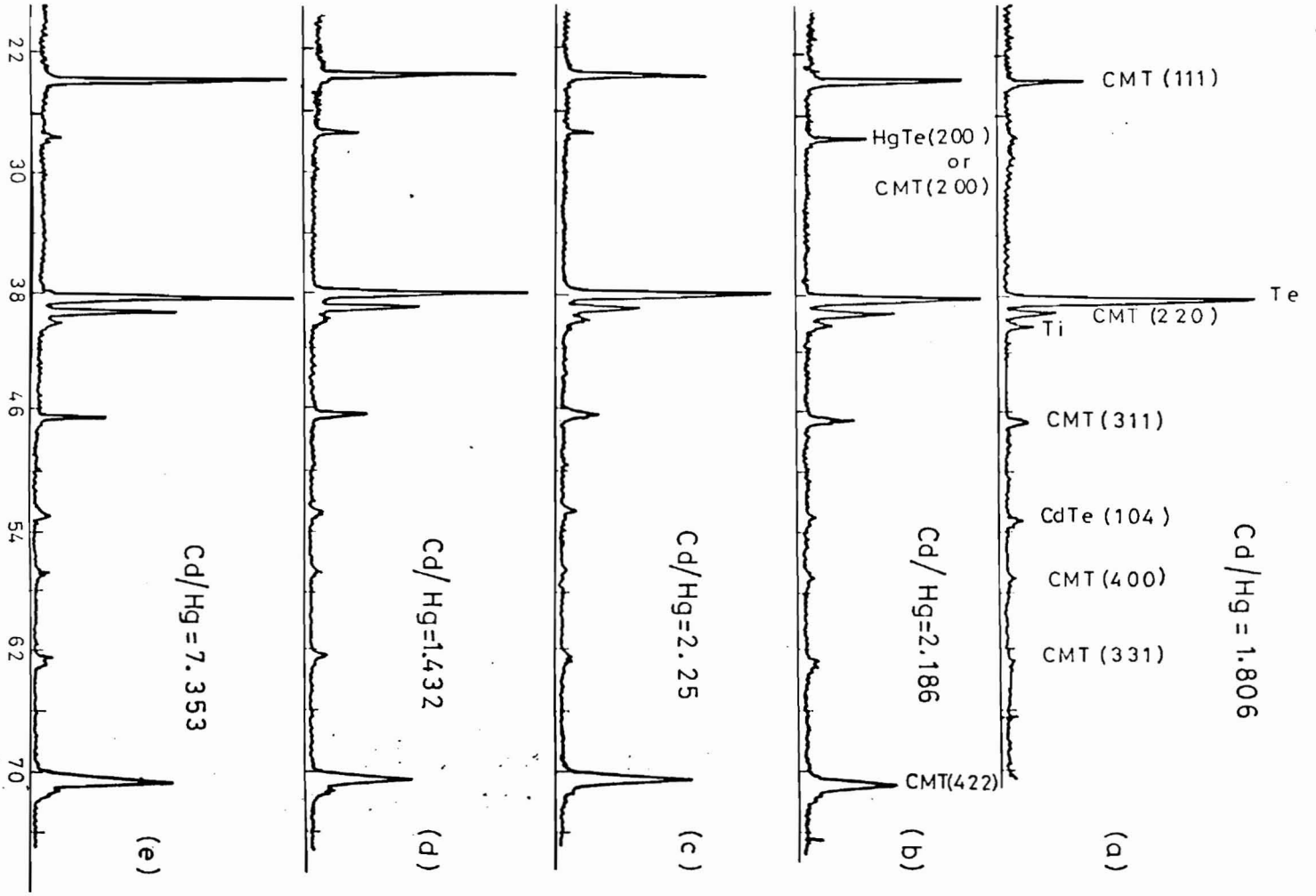
CMT (111)
HgTe(200)
or
CMT(200)
Te
CMT (220)
Ti
CMT (311)
CdTe (104)
CMT (400)
CMT (331)
CMT(422)
Cd/Hg = 1.806
Cd/Hg=2.186
Cd/Hg=2.25
Cd/Hg=1.432
Cd/Hg=7.353
(a)
(b)
(c)
(d)
(e)
22
30
38
46
54
62
70

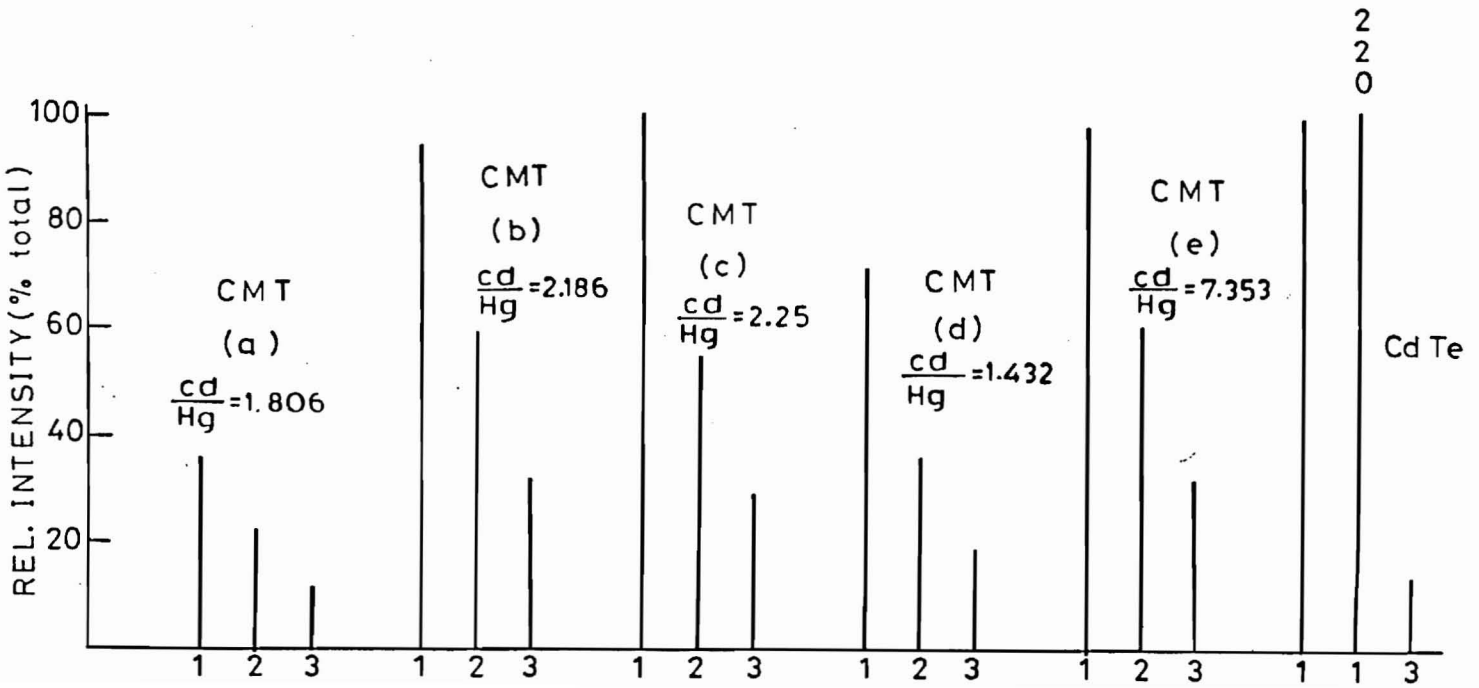
REL. INTENSITY (% total)
100
80
60
40
20
CMT
(a)
cd/Hg = 1.806
CMT
(b)
cd/Hg = 2.186
CMT
(c)
cd/Hg = 2.25
CMT
(d)
cd/Hg = 1.432
CMT
(e)
cd/Hg = 7.353
220
Cd Te
1 2 3
1 2 3
1 2 3
1 2 3
1 2 3
1 1 3

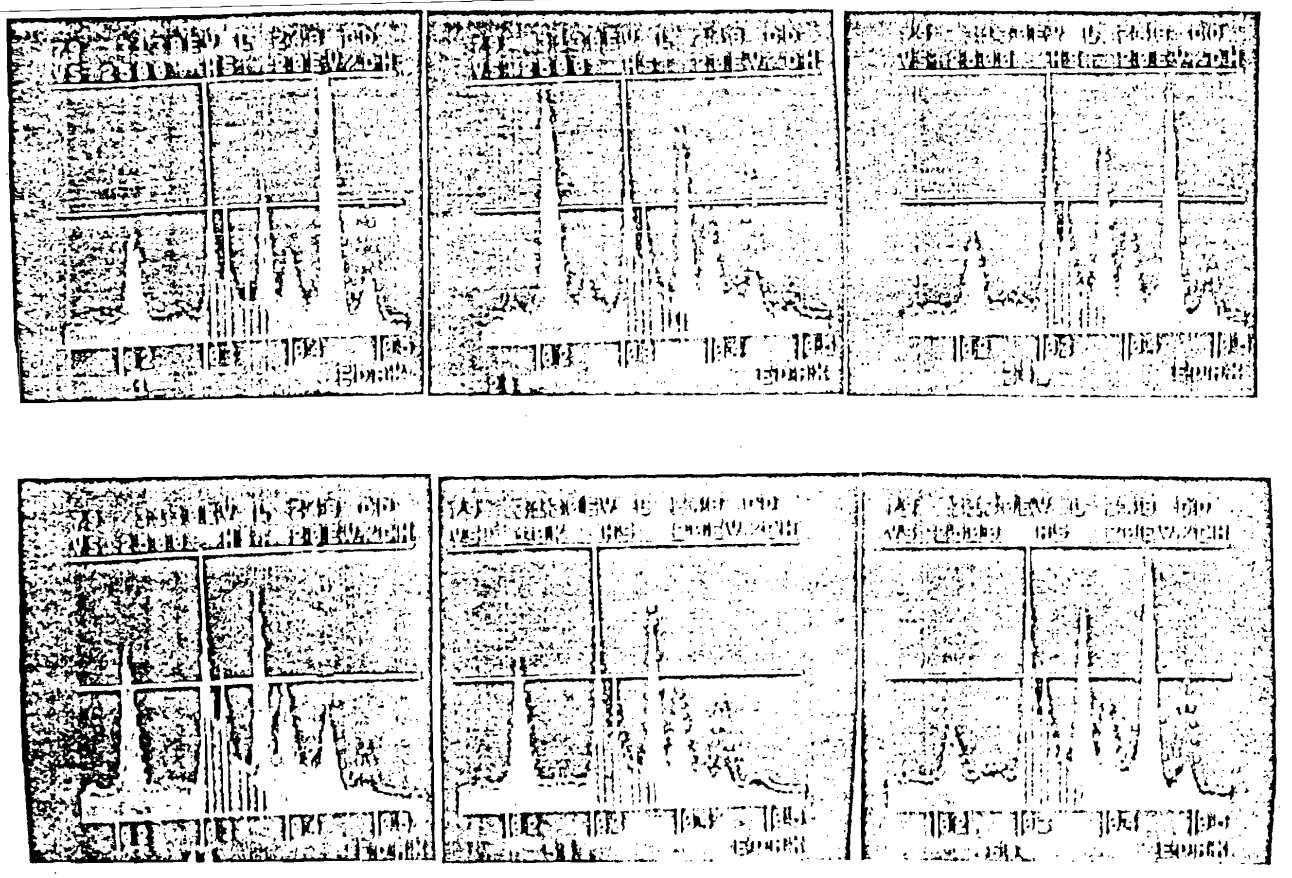

Fig-3

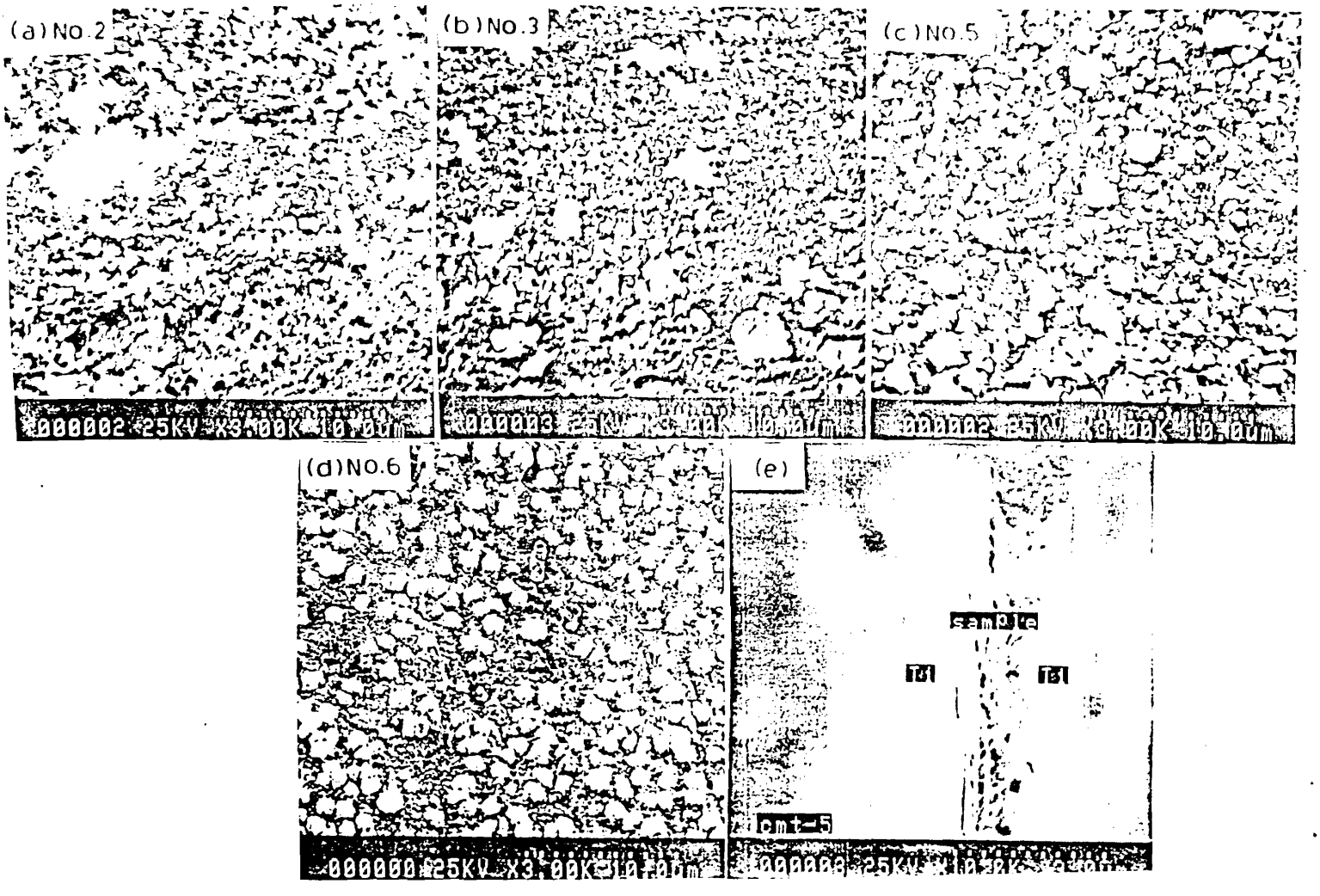

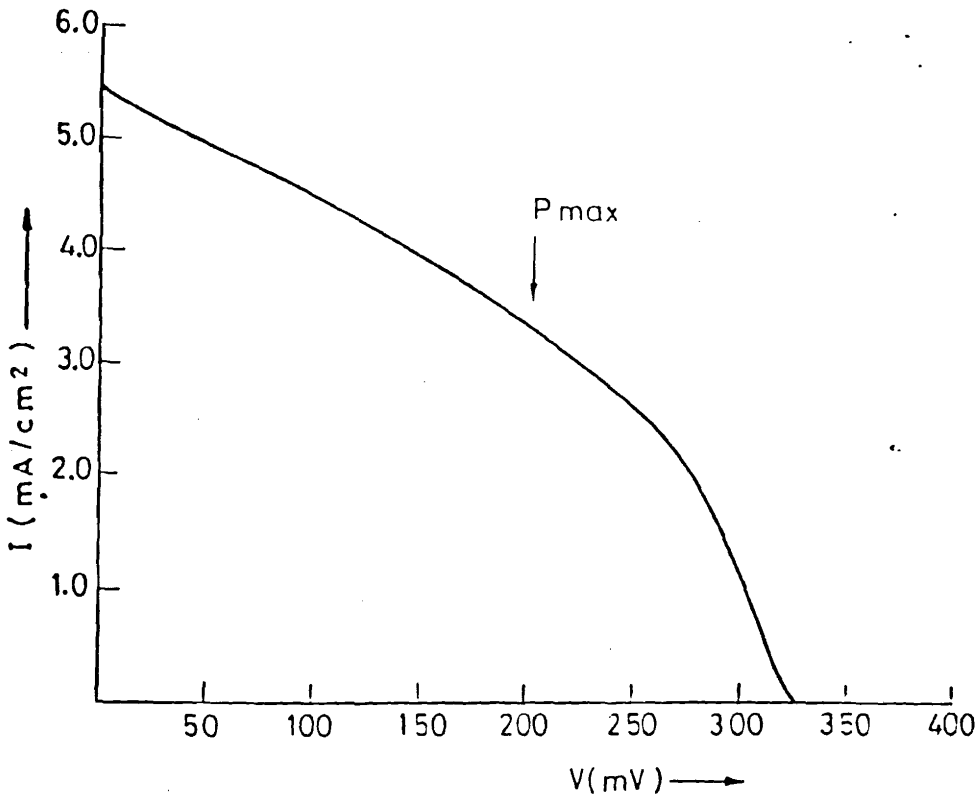

Fig. 11